

## Torus quantization of symmetrically excited helium

Jörg Müller

*Department of Physics, University of Tennessee, Knoxville, Tennessee 37996-1200*

Joachim Burgdörfer

*Department of Physics, University of Tennessee, Knoxville, Tennessee 37996-1200  
and Oak Ridge National Laboratory, Oak Ridge, Tennessee 37831-6377*

Donald Noid

*Oak Ridge National Laboratory, Oak Ridge, Tennessee 37831-6377*

(Received 29 July 1991)

The recent discovery by Richter and Wintgen [J. Phys. B **23**, L197 (1990)] that the classical helium atom is not globally ergodic has stimulated renewed interest in its semiclassical quantization. The Einstein-Brillouin-Keller quantization of Kolmogorov-Arnold-Moser tori around stable periodic orbits becomes locally possible in a selected region of phase space. Using a hyperspherical representation we have found a dynamically confining potential allowing for a stable motion near the Wannier ridge. The resulting semiclassical eigenenergies provide a test for full quantum calculations in the limit of very high quantum numbers. The relations to frequently used group-theoretical classifications for doubly excited states and to the periodic-orbit quantization of the chaotic portion of the phase space are discussed. The extrapolation of the semiclassical quantization to low-lying states give remarkably accurate estimates for the energies of all symmetric  $L=0$  states of helium.

PACS number(s): 03.65.Sq, 31.50.+w, 31.20.Tz

### I. INTRODUCTION

The apparent failure of the "old quantum theory" in the early 1920s to describe three-body Coulomb systems such as helium and  $H_2^+$  has decisively stimulated the development of the modern quantum theory embodied in the Schrödinger equation. As first recognized by Leopold and Percival only about 10 years ago [1] the failure of the old quantum theory was not due to the semiclassical approximation underlying Bohr-Sommerfeld-type quantization itself but due to its incomplete implementation. Specifically essential ingredients of modern semiclassical theory, such as the Maslov indices for conjugate points of classical trajectories, were missing [2]. Clearly, the role of the latter could be appreciated only after semiclassical mechanics was understood as the short-wavelength limit of wave mechanics. Using perturbation theory and variational optimization, Leopold and Percival could give a reasonable estimate for the binding energy of the ground state of He. A complete semiclassical theory of helium is, however, still missing.

The renewed interest in semiclassical methods is stimulated by recent observations of highly doubly excited states [3–6] with principal quantum numbers of the two electrons (within an independent particle model) of up to 80. A full quantum description appears to be still out of reach for the most sophisticated calculations presently available [7–10]. In this regime, the semiclassical approximation is expected to be valid and, possibly, easier to apply.

One major obstacle in implementing semiclassical methods is the complete breakdown of the independent

particle approximation. Since the experimental identification of low-lying doubly excited states [11], it was recognized [12] that their existence hinges on a highly correlated motion of the two electrons maintaining a delicate balance of repulsive and attractive fields. The strength of electron-electron correlation prevents a description in terms of a perturbation theory for weakly perturbed Kepler orbits [13]. Furthermore, the classical phase space for the three-body Coulomb problem is largely chaotic. The Einstein-Brillouin-Keller (EBK) quantization of invariant Kolmogorov-Arnold-Moser (KAM) tori is therefore *globally* not applicable. In fact, it was widely believed that classical Helium would be unstable apart from the set of initial conditions of measure zero, and would spontaneously autoionize [14].

Recently, however, Richter and Wintgen [15] discovered that the phase space near the so-called Langmuir orbit [16] is stable. The Langmuir orbit is one of the periodic orbits suggested in the early 1920s as possible candidates for the Bohr-Sommerfeld quantization (for historic details see Refs. [1] and [2]). The importance of this discovery lies in the fact that for a stable island around a periodic orbit, rigorous torus quantization becomes *locally* possible provided the size of the island is of the order of  $\hbar^m$  ( $m$  is the number of degrees of freedom) such as to support at least one quantum state [17]. The Langmuir orbit is isolated, i.e., no periodic-orbit-preserving continuous transformation on a given energy shell exists. In view of the Gutzwiller trace formula for periodic-orbit quantization [2], the Langmuir orbit will also contribute to the spectral fluctuation of the quantum system, when the surrounding phase space is insufficient

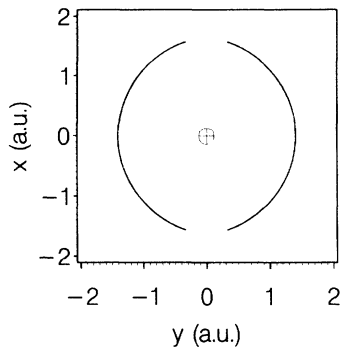


FIG. 1. The Langmuir orbit (LO) at  $E = -1$  a.u. The nucleus ( $Z=2$ ) is located at the origin.

to support discrete quantum states. Major progress has been recently achieved in enumerating unstable periodic orbits of the chaotic phase-space region of He [18,19].

In the following we present the EBK quantization of the phase space in the vicinity of the Langmuir orbit. The resulting eigenenergies pertain to symmetrically ( $n_1 \approx n_2 \gg 1$ ) highly excited Helium.  $n_1$  and  $n_2$  are the principal quantum numbers of the individual electrons. In the following the notation  $N = \min(n_1, n_2)$  and  $n = \max(n_1, n_2)$  will be used. We discuss extrapolation to lower  $N$  and relate the semiclassical quantum numbers with the approximate  $O(4)$  quantum numbers [20]  $(NKTn)^4$  to the so-called Wannier “ridge-riding” states. Atomic units are used throughout unless otherwise indicated.

## II. CONFINING POTENTIAL FOR THE LANGMUIR ORBIT

In 1921 Langmuir [16] suggested a planar configuration with two electrons performing bending vibrations as a possible classical realization of a two-electron orbit with total quantum number  $L=0$  (Fig. 1). This periodic Langmuir orbit (LO) represents a collective, completely correlated motion of two equivalent elec-

trons, distinctly different from any independent particle motion on (distorted) Kepler orbits. The significance of the LO results, in part, from the fact that in a limited interval of nuclear charges  $Z$  around  $Z = 2$ , the LO is linearly stable [15].

The torus quantization of the stable island around the LO can be most conveniently performed in the hyperspherical representation pioneered by Macek [21]. The Hamiltonian for Helium with infinite nuclear mass and  $L=0$  is given in hyperspherical coordinates by

$$H = \frac{1}{2} \left[ p_R^2 + \frac{p_\alpha^2}{R^2} + \frac{p_\theta^2}{R^2 \sin^2 \alpha \cos^2 \alpha} \right] + \frac{\Gamma(\alpha, \theta)}{R} \quad (1)$$

with the hyperspherical potential

$$\Gamma(\alpha, \theta) = \frac{1}{\sqrt{1 - \sin 2\alpha \cos \theta}} - \frac{Z}{\sin \alpha} - \frac{Z}{\cos \alpha}, \quad (2)$$

where  $Z=2$  for helium.  $R = (r_1^2 + r_2^2)^{1/2}$  is the hyperradius,  $\alpha = \arctan(r_2/r_1)$  is called the hyperangle,  $\theta$  is the angle between the electrons, and  $r_i$  is the distance of the  $i$ th electron to the nucleus.  $p_R$ ,  $p_\alpha$ , and  $p_\theta$  are the canonically conjugated momenta.

Equation (1) describes a Hamiltonian dynamical system with three degrees of freedom. The energy hypersurface is five dimensional (5D) and tori, or remnants thereof, constitute three-dimensional manifolds embedded in the energy hypersurface. It is important to realize that ordinary 2D Poincaré surface of sections do not fully represent tori in systems with three (or more) degrees of freedom. The latter leads to complications for the quantization of stable islands, as will be discussed below.

The classical three-body Coulomb problem possesses, like the two-body problem, a scaling invariance with respect to the total energy  $E$  (Kepler’s law), i.e., the equations of motion are invariant under a continuous mechanical similarity transformation, by which the energy (and characteristic length and time scales) is continuously changed. It is therefore sufficient to perform all classical calculations at a fixed energy  $E = -1$  a.u. This scaling invariance is broken in quantum mechanics due to the existence of a fundamental scale (via  $\hbar$ ). However, for clas-

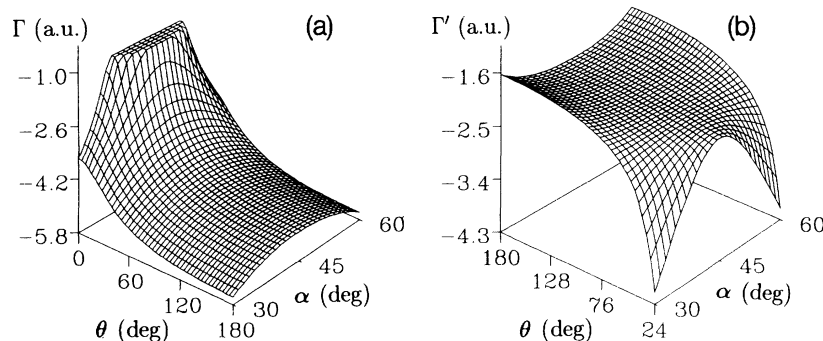


FIG. 2. (a) Potential  $\Gamma(\alpha, \theta)$  in hyperspherical coordinates. [Due to the singularity at  $(\alpha = \pi/4, \theta = 0^\circ)$  values of  $\Gamma > -1$  are set to  $-1$ .] (b) Effective potential  $\Gamma'(\alpha, \theta)$  in hyperspherical coordinates. ( $\Gamma'$  is not defined for angles  $\theta < \theta_{\min} \approx 24^\circ$ , since this region is classically forbidden.)

sically regular motion the corresponding quantum spectrum possesses a discrete scaling invariance [22,23], very much like the discrete translation symmetry on a lattice.

The Langmuir orbit resides on the Wannier ridge ( $\alpha = \pi/4$  or  $r_1 = r_2$ ). The equilibrium position of the bending oscillation ( $\theta = \pi$ ) is located at the hyperradius  $R_0(E = -1) = 1.989883, \dots$ , a.u. Figure 2(a) displays the by now well-known hyperspherical representation of the potential  $\Gamma(\alpha, \theta)/R$ . Because of the presence of the saddle it was widely believed that the motion would be unstable [14]. The linear stability [15] of the LO indicates however the dynamical stabilization of the orbit. In Fig. 2(b) we present the hyperspherical representation of the dynamically confining potential in the vicinity of the Langmuir orbit

$$\frac{\Gamma'(\alpha, \theta)}{R} = \frac{1}{R} \left[ \Gamma(\alpha, \theta) + \frac{p_\theta^2}{R \sin^2 \alpha \cos^2 \alpha} \right]. \quad (3)$$

The confining potential constitutes the analog of the centrifugal potential for the two-body problem. In contrast to the centrifugal potential, the corresponding correction term in (3) does not only contain constants of motion and depends therefore on the trajectory, i.e.,  $p_\theta$  and  $R$  are functions of  $\theta$ . For the LO itself they are independent of  $\alpha$  since  $\alpha = \pi/4$  is constant. Elongations around the LO ( $\delta_\alpha = \alpha - \pi/4$ ) will introduce an  $\alpha$  dependence of  $p_\theta$  and  $R$ . However, these modifications can be neglected for orbits sufficiently close to the LO since they affect the coefficient of the lowest-order correction ( $\propto \delta_\alpha^2$ ) in a Taylor expansion of  $\Gamma'(\alpha, \theta \approx \pi)$  around  $\alpha = \pi/4$  only by a few percent.

The Hamiltonian can now be written in the form

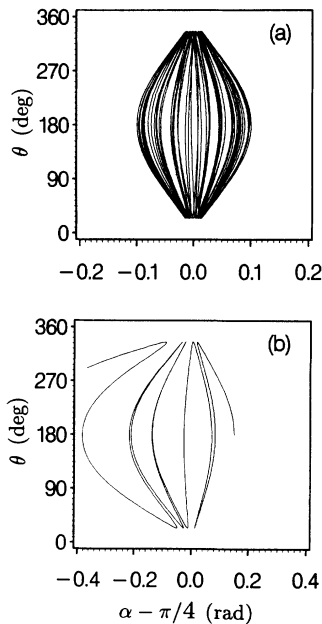


FIG. 3. Trajectories of classical helium in hyperspherical coordinates. Initial conditions:  $E = -1$  a.u.,  $L = 0$ ,  $\theta = \pi$ ,  $R = R_0$ ,  $p_R = 0$ ,  $p_\alpha = 0$ . (a)  $\epsilon = \alpha - (\pi/4) = 0.01$ , (b)  $\epsilon = \alpha - (\pi/4) = 0.015$ .

$$H_{\text{eff}} = \frac{p_\alpha^2}{2R^2} + \frac{p_R^2}{2} + \frac{\Gamma'(\alpha, \theta)}{R(\theta)}. \quad (4)$$

The effective potential  $\Gamma'(\alpha, \theta)/R(\theta)$  [Fig. 2(b)] allows for bounded motion in the  $\alpha$  direction. The  $\theta$  dependence of  $\Gamma'$  or  $H_{\text{eff}}$  can be viewed as a time-dependent potential with  $\theta(t)$  given by the periodic orbit. During one period the electrons will feel a restoring force towards  $\alpha = \pi/4$  when  $\theta$  is larger than a critical angle  $\theta_{\text{crit}}$  (in the case of helium approximately  $70^\circ$ ), whereas the system will be driven away from  $\alpha = \pi/4$  when  $\theta$  ranged from  $\theta_{\text{crit}}$  to  $\theta_{\text{min}}$  (approximately  $24^\circ$  for He). The restoring force is due to the momentum in the  $\theta$  direction  $p_\theta$  which is small for small angles  $\theta$ . As shown in Fig. 3(a) we find bounded motion for small elongation in the  $\alpha$  direction. However, when the elongation is too large, the trajectory stays only for a finite time close to the LO and the system will eventually autoionize [Fig. 3(b)].

These results remain qualitatively unchanged for realistic values for the finite mass of the nucleus. Only when the electron mass becomes close to the nuclear mass (e.g., muonic helium), the stable region disappears. It is instructive to relate the Langmuir orbit to other frequently employed periodic orbits representing collective motion of the two-electron system. The so-called ‘‘Wannier orbit’’ [24] (‘‘symmetric stretch’’) for the electrons moving in-phase radially (inward) outward on opposite sides of the nucleus ( $\mathbf{r}_1 = -\mathbf{r}_2$ ) corresponds to a fixed point in the  $\alpha$ - $\theta$  plane [Fig. 4(a)] and to a line along the diagonal in

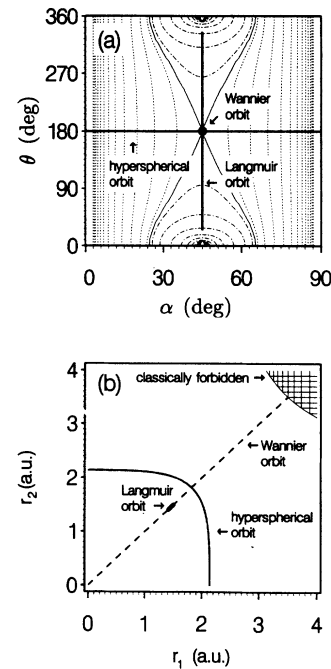


FIG. 4. Three fundamental periodic orbits for the two-electron problem ( $E = -1$  a.u.): symmetric stretch (Wannier orbit), asymmetric stretch (hyperspherical orbit), and Langmuir orbit in (a) the  $\theta$ - $\alpha$  plane [contour lines of  $\Gamma(\alpha, \theta)$  are overlaid] and (b) the  $r_1$ - $r_2$  plane. (The Wannier orbit corresponds to a fixed point in the  $\theta$ - $\alpha$  plane.)

the  $r_1$ - $r_2$  plane including the origin [Fig. 4(b)] and is therefore strongly unstable [15]. The projection of the “asymmetric stretch” or hyperspherical (out of phase) mode [25] is near-circular in an  $r_1$ - $r_2$  plane while it corresponds to a horizontal line in the  $(\theta, \alpha)$  plane. As pointed out by Watanabe [25] and by Ezra and co-workers [18,19] the low-lying symmetrically ( $N=n$ ) excited states with the state label ( $K=K_{\max}=N-1$ ,  $A=+$ ) trace the weakly unstable hyperspherical rather than the Wannier orbit. The probability distribution for those states [19,26] clearly shows that the motion is transverse to rather than along the Wannier ridge. The density enhancement near the ridge ( $\alpha=\pi/4$ ) can be easily understood semiclassically noting that

$$|\psi(\alpha)|^2 \propto |v(\alpha)|^{-1}, \quad (5)$$

where  $v(\alpha)$  is the local speed along the periodic orbit. At the saddle, where the potential reaches its maximum along the asymmetric stretch orbit, the motion slows down, leading to a density enhancement.

The Langmuir orbit, on the other hand, corresponds to the motion along the ridge. The excursion in the  $\alpha$  direction,  $\delta_\alpha = \alpha - \pi/4$ , and along the hyperradius,  $\delta_R = R - R_0$ , is small while the amplitude of the bending motion along  $\theta$  is, in general, large. Based on this observation we conjecture that quantum states, localized near the Langmuir orbit, will correspond, for highly excited He, to high-lying states within the intrashell manifold with  $K \approx K_{\min} = -(N-1)$ .

### III. QUANTIZATION OF THE LANGMUIR ORBIT

The immediate vicinity of the Langmuir orbit forms a stable resonant island in phase space. Locally, tori exist for  $|\delta_R| = |R - R_0| < 0.05$  and  $|\delta_\alpha| = |\alpha - \pi/4| < \delta_{\alpha, \max} = 0.13$ . Isolated resonant islands can then be quantized in close analogy to integrable systems where  $m$  constants of motion exist in involution.

Our method of torus quantization utilizes integration along invariant curves on the Poincaré surface of section [17]. The quantization of each torus requires the actions along three topologically distinct paths:

$$\begin{aligned} S_\theta &= \oint_{P_1} \mathbf{p} \cdot d\mathbf{q}, \\ S_\alpha &= \oint_{P_2} p_\alpha d\alpha, \\ S_R &= \oint_{P_3} p_R dR. \end{aligned} \quad (6)$$

$P_1$  is given by the trajectory itself. For periodic trajectories  $P_1$  is closed, however, in the case of quasiperiodic trajectories the endpoints have to be connected on the torus.  $P_2$  is defined as the intersection of the torus with the hypersurface  $\theta = \pi$  and  $p_R = 0$  and, accordingly,  $P_3$  is the intersection with  $\theta = \pi$  and  $p_\alpha = 0$ .

The action  $S_\theta$  along the trajectory ( $P_1$ ) is computed while solving Hamilton’s equations of motion. In order to obtain the actions  $S_\alpha$  and  $S_R$  along  $P_2$  and  $P_3$  we record a large number of intersections (typically 1000 to 3000) of the trajectory with the hyperplane  $\theta = \pi$ . Out of these intersections, a relatively small number (typically

100) with the smallest values of  $|p_R|$  (or  $|p_\alpha|$ ) are chosen to construct “fuzzy” Poincaré maps (Fig. 5). There are no sharp lines, in contrast to Poincaré maps for two-dimensional systems. The finite width of the lines is due to the fact that the momenta  $p_R$  or  $p_\alpha$  at the intersections are not equal to zero. The width is proportional to the average deviation of these momenta from zero. The hyperspherical coordinates are then transformed to action-angle variables. The action integrals are evaluated according to the methods described in Ref. [27].

We use a grid of 500 points in the  $\delta_R$ - $\delta_\alpha$  plane. Whereas the actions  $S_R$  and  $S_\alpha$  show, to a good degree of approximation, a quadratic dependence on  $\delta_R$  and  $\delta_\alpha$ , the action along the orbit contains significant anharmonic corrections. We find

$$\begin{aligned} S_\theta(\delta_R, \delta_\alpha) &= S_0 + a_1 \delta_\alpha^4 + a_2 \delta_\alpha^2 \delta_R^2 + a_3 \delta_R^4, \\ S_\alpha(\delta_\alpha) &= a_4 \delta_\alpha^2, \\ S_R(\delta_R) &= a_5 \delta_R^2, \end{aligned} \quad (7)$$

where  $S_0 = 16.991418, \dots$ , a.u. is the action of the LO. The best fit (minimal relative deviation) for the parameters  $a_i$  are  $a_1 = -0.382 \pm 0.001$ ,  $a_2 = 10.0 \pm 0.5$ ,  $a_3 = -0.0448 \pm 0.0003$ ,  $a_4 = 0.232 \pm 0.001$ , and  $a_5 = 3.27 \pm 0.01$ . The errors are obtained by varying the weights of the individual deviations of  $|S_\theta(\delta_\alpha(j), \delta_R(j)) - S_\theta^{\text{fit}}(\delta_\alpha(j), \delta_R(j))|$  where  $j$  refers to one of the 500

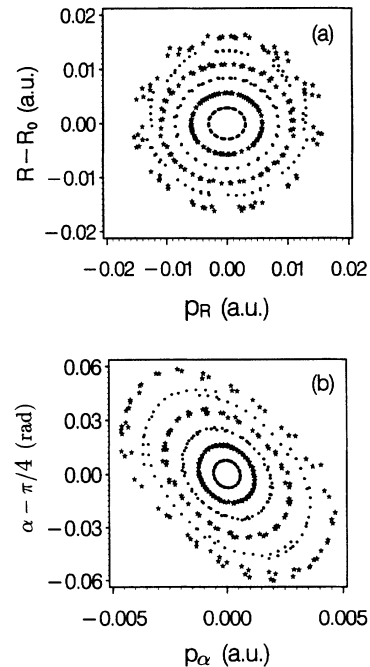


FIG. 5. Projected Poincaré maps in a four-dimensional space at  $\theta = \pi$ . (a)  $p_\alpha \approx 0$ , (b)  $p_R \approx 0$ . Out of 1000 intersections with  $\theta = \pi$  for each trajectory only the 70 intersections with the smallest  $p_i$  are used. Initial conditions:  $E = -1$  a.u.,  $L = 0$ ,  $\theta = \pi$ ,  $p_R = 0$ ,  $R_0 + \delta_R$ ,  $\alpha = (\pi/4) + \delta_\alpha$  with  $\delta_\alpha = 2.5\delta_R$ . Trajectories with  $\delta_R = 0.003, 0.009$ , and  $0.015$  are denoted by  $\bullet$  and those with  $\delta_R = 0.006, 0.012$ , and  $0.018$  are denoted by  $*$ .

points in the  $\delta_\alpha$ - $\delta_R$  plane.

The EBK quantization conditions for the actions are now

$$\begin{aligned} S'_\theta &= 2\pi[n_\theta + 1 + \gamma_R(n_R + \frac{1}{2}) + \gamma_\alpha(n_\alpha + \frac{1}{2})], \\ S'_\alpha &= 2\pi(n_\alpha + \frac{1}{2}), \\ S'_R &= 2\pi(n_R + \frac{1}{2}), \end{aligned} \quad (8)$$

where  $n_\theta$ ,  $n_\alpha$ , and  $n_R$  are the semiclassical quantum numbers.  $\gamma_\alpha = \omega_\alpha/\omega_\theta$  and  $\gamma_R = \omega_R/\omega_\theta$  are the winding numbers which are the ratios of the frequencies of the oscillations in the  $\theta$ ,  $R$ , and  $\alpha$  directions. They are calculated during the evaluation of the actions  $S_\alpha$  and  $S_R$  since they describe the change of the action variable of the  $\alpha$  or  $R$  motion during one cycle of the  $\theta$  motion. The winding numbers are given up to second order in  $\delta_\alpha$  and  $\delta_R$  by

$$\begin{aligned} \gamma_R &= \gamma_R^0 + \gamma_R^\alpha \delta_\alpha^2 + \gamma_R^R \delta_R^2 \\ &= 0.8808 + 3.95\delta_\alpha^2 + 0.18\delta_R^2, \\ \gamma_\alpha &= \gamma_\alpha^0 + \gamma_\alpha^\alpha \delta_\alpha^2 + \gamma_\alpha^R \delta_R^2 \\ &= 0.1960 - 3.97\delta_\alpha^2 + 47.74\delta_R^2. \end{aligned} \quad (9)$$

In order to satisfy the quantization conditions (8), the classical actions (7) which are calculated for  $E = -1$  a.u. have to be rescaled involving the similarity transformation

$$S' = \beta S \quad (10)$$

which, in turn, determines the energy

$$E' = -\beta^{-2} = -\left[\frac{S}{S'}\right]^2. \quad (11)$$

Combining Eqs. (7)–(11) we find the semiclassical energy eigenvalues pertaining to the Langmuir orbit

$$E(n_\theta, n_\alpha, n_R) = -\left[\frac{S_0}{2\pi[n_\theta + 1 + \lambda(n_\alpha, n_R)]}\right]^2 \left[\frac{1}{2} + \left[\frac{1}{4} - \frac{\Lambda(n_\alpha, n_R)}{[n_\theta + 1 + \lambda(n_\alpha, n_R)]^2}\right]^{1/2}\right]^{-2} \quad (12)$$

with

$$\lambda(n_\alpha, n_R) = \gamma_\alpha^0 \left[n_\alpha + \frac{1}{2}\right] + \gamma_R^0 \left[n_R + \frac{1}{2}\right], \quad (13)$$

$$\begin{aligned} \Lambda(n_\alpha, n_R) &= \bar{\mu}_\alpha \left[n_\alpha + \frac{1}{2}\right]^2 + \bar{\nu}_{\alpha,R} \left[n_\alpha + \frac{1}{2}\right] \left[n_R + \frac{1}{2}\right] \\ &\quad + \bar{\mu}_R \left[n_R + \frac{1}{2}\right]^2 \end{aligned} \quad (14)$$

and with constants

$$\begin{aligned} \bar{\mu}_\alpha &= \frac{S_0}{a_4^2} (a_1 - a_4 \gamma_\alpha^\alpha), \\ \bar{\nu}_{\alpha,R} &= \frac{S_0}{a_4 a_5} (a_2 - a_4 \gamma_\alpha^R - a_5 \gamma_R^\alpha), \\ \bar{\mu}_R &= \frac{S_0}{a_5^2} (a_3 - a_5 \gamma_R^R). \end{aligned} \quad (15)$$

$n_\theta$  is the quantum number of the (high) excitation of the bending oscillation and thus counts the nodes along the LO. Since the number of nodes is identical for both electrons,  $n_\theta$  has to be even.  $n_\alpha$  is the quantum number of the asymmetric stretch oscillation and  $n_R$  the quantum number of the oscillation of the hyperradius (Wannier mode).

The first term of Eq. (12) corresponds to the harmonic oscillations. Only the action  $S_0$  as well as the winding numbers  $\gamma_\alpha^0$  and  $\gamma_R^0$  enter here. The second term containing the square root describes the anharmonicity and couplings between the different vibrational modes (it converges to 1 in the limit  $n_\theta \gg n_\alpha, n_R$ ).

Since the size of the stable region is very small, the

zero-point oscillation transverse to the orbit with action  $\pi/2$  “fits” into the island only for large scaling constants  $\beta$ ,

$$\beta \geq 2.15 \frac{\pi}{\delta_{\alpha,\max}^2}. \quad (16)$$

Therefore, the action along the orbit, and hence  $n_\theta$ , must be very large,  $n_\theta > 10^3$ , i.e.,  $N > 5 \times 10^2$ . States with such large quantum numbers have not yet been experimentally reached. The largest principal quantum numbers currently accessible for symmetrically excited states [28] are of the order of  $N \approx 1 \times 10^2$ . States described by Eqs. (12)–(15) would correspond to extremely long-lived states that are stable against classical autoionization and whose only decay mode would be either radiative or tunneling through the barrier set up by the dynamically confining potential [Fig. 2(b)]. The extrapolation to lower-lying states will be discussed in Sec. IV.

Using the close correspondence between the quantum numbers for collective modes of a triatomic molecule and the frequently used group-theoretical quantum numbers [20,29] assigned to doubly excited states  $(NK\tau n)^A$ , we are led to the following identification for the  $L=0$  singlet states ( $^1S$ ), i.e.,  $A = +$ :

$$\begin{aligned} N &= \frac{1}{2}(n_\alpha + n_\theta + 2), \\ K &= \frac{1}{2}(n_\alpha - n_\theta). \end{aligned} \quad (17)$$

The singlet states ( $^1S$ ) are characterized by an antinode at  $\alpha = \pi/4$  (i.e.,  $r_1 = r_2$ ), whereas the triplet wave functions show a node at  $\alpha = \pi/4$ . This implies that  $n_\alpha$  is even for ( $^1S$ ) and odd for ( $^3S$ ) states [ $A = (-1)^{n_\alpha}$ ]. Correspondingly, we find for ( $^3S$ ), i.e.,  $A = -$

$$N = \frac{1}{2}(n_\alpha + n_\theta + 1), \quad (18)$$

$$K = \frac{1}{2}(n_\alpha - n_\theta - 1)$$

and for both cases  $n$  is given by

$$n = N + n_R. \quad (19)$$

The quantum number  $n_R$  can become zero only for singlet states, since intrashell states ( $N=n$ ) always have  $A=+$ . Furthermore  $T=0$  since  $L=0$ .

Thus we can rewrite Eq. (12) using the group-theoretical quantum numbers  $N$ ,  $n$ , and  $K$ . In the limit of large  $N$

$$E(N, n, K) = -\frac{\left[\frac{S_0}{4\pi}\right]^2}{(N-\mu)^2} \left[ 1 - \frac{1}{2}(\gamma_\alpha^0 - 1) \left[ 1 + \frac{K}{N} \right] - \gamma_R^0 \left[ \frac{n-N}{N} \right] + O(N^{-2}) \right]^2 \quad (20)$$

with

$$\mu = \frac{1}{4}(\gamma_\alpha^0 - \gamma_R^0).$$

Equation (20) is valid in the limit  $N \rightarrow \infty$ ,  $K/N \rightarrow -1$ , and  $n/N \rightarrow 1$ .

#### IV. EXTRAPOLATION TO LOW-LYING STATES

The rigorous torus quantization presented above has the obvious drawback that it provides only a subset of eigenenergies in the asymptotic limit of high quantum numbers very close to the double-ionization threshold associated with classically stable orbits. It is therefore tempting to extrapolate Eq. (20) to lower  $N$  where the size of the regular island in phase space will be less than  $\hbar^3$  and thus too small to support a quantum-mechanical state.

The only known semiclassical quantization method for largely chaotic systems is the Gutzwiller trace formula [2] or variants thereof. Rather than individual eigenenergies, periodic-orbit quantization describes resonances, i.e., fluctuations in the spectral densities due to the influence of unstable periodic orbits. However, the application of the trace formula to mixed systems with regular and chaotic regions in phase space proves much more difficult. Ezra *et al.* [19] have recently succeeded in the coding of all unstable periodic orbits which are relatives of the asymmetric stretch orbit up to symbolic length 6.

We discuss in the following a much simpler but less rigorous approach which appears to be remarkably successful in describing approximate positions of all intrashell resonances of He with total angular momentum  $L=0$ .

Our extrapolation is based on three key observations. (a) The top and the bottom end of the intrashell manifolds for symmetric double excitation are associated with stable periodic Langmuir and weakly unstable periodic asymmetric-stretch orbits, respectively. Resonances belonging to an intrashell manifold should therefore be

strongly influenced by the properties of these two “limiting” orbits. (b) Each classical periodic orbit is, to leading order [see Eq. (12)], described by its action and the winding numbers for the vibrations in the corresponding transverse hyperplane of stable motion. These parameters are expected to determine the position of resonances. The Lyapunov exponent of unstable orbits will primarily influence their width. (c) Based on the classical scaling invariance [Eq. (11)], the position of intrashell resonances ( $n=N$ ) can be written as [30] (the “grandparent model”)

$$E(N, N, K) = -\frac{Z_{\text{eff}}^2 \left[ \frac{K}{N} \right]}{N^2} \quad (21)$$

neglecting the quantum defect  $\mu$  [31]. Thus in the semiclassical limit  $Z_{\text{eff}}$  does not depend on  $K$  and  $N$  separately, but only on their ratio. Similar dependence on scaled quantum numbers has also been found in other systems [23].

The function  $Z_{\text{eff}}$  can now be determined if we impose the requirements that in the limit of large  $N$  and  $K \simeq K_{\text{min}}$ ,  $Z_{\text{eff}}$  reproduces the classical action and winding numbers of the Langmuir orbit and for  $K \simeq K_{\text{max}}$  those of the asymmetric stretch. The effective charge  $Z_{\text{eff}}$  must therefore satisfy

$$\lim_{N \rightarrow \infty} \lim_{K/N \rightarrow -1} Z_{\text{eff}} \left[ \frac{K}{N} \right] = \frac{S_0}{4\pi} \left[ 1 - \frac{\gamma_\alpha^0 - 1}{2} \left[ 1 + \frac{K}{N} \right] \right], \quad (22)$$

$$\lim_{N \rightarrow \infty} \lim_{K/N \rightarrow 1} Z_{\text{eff}} \left[ \frac{K}{N} \right] = \frac{S_{\text{as}}}{4\pi} \left[ 1 - \frac{\gamma_\theta - 1}{2} \left[ 1 - \frac{K}{N} \right] \right], \quad (23)$$

where  $S_{\text{as}} = 22.986$  and  $\gamma_\theta = 1.0785$  are the action and the winding number of the asymmetric stretch at  $E = -1$  a.u.

The simplest smooth-function interpolation between Eqs. (22) and (23) which depends only on the classical orbital parameters and contains no free parameters is given by a third-order polynomial in  $K/N$ . Its four coefficients are completely determined by the two actions and two winding numbers of the limiting orbits

$$Z_{\text{eff}} \left[ \frac{K}{N} \right] = 1.708 + 0.204 \left[ \frac{K}{N} \right] - 0.118 \left[ \frac{K}{N} \right]^2 + 0.035 \left[ \frac{K}{N} \right]^3. \quad (24)$$

By construction, Eq. (24) converges to the limiting cases Eqs. (22) and (23). It also converges to the result for the torus quantization [Eq. (20)] in the intrashell case  $N=n$ .

The choice of the interpolation formula [Eq. (24)] is somewhat arbitrary. Any strictly monotonic and smooth function with four free parameters [determined by Eqs. (22) and (23)] is admissible. However, we find that changes of the interpolation formula affect the results (see Table I) only at the level of 1%.

Table I compares the predicted position of the reso-

TABLE I. Eigenenergies of intrashell  $^1S$  resonances of helium (in a.u.). The results of the extrapolation formula [Eqs. (21) and (24)] are compared to accurate quantum calculations.

$K/N$	$N$	$K$	Present work	Ref. [7]	Ref. [9]	Ref. [19]	Ref. [26]
0.000	1	0	2.9173		2.8954	2.904	2.8911
0.500	2	1	0.7964	0.7787	0.7721	0.778	0.7731
-0.500	2	-1	0.6179	0.6053	0.6219		
0.667	3	2	0.3608	0.3535	0.3529	0.354	0.3529
0.000	3	0	0.3241	0.3175	0.3072		
-0.667	3	-2	0.2531	0.2551	0.2574		
0.750	4	3	0.2046	0.2010	0.2012	0.201	0.2013
0.250	4	1	0.1919	0.1878	0.1833		
-0.250	4	-1	0.1700	0.1683	0.1633		
-0.750	4	-3	0.1358	0.1411			
0.800	5	4	0.1316	0.1294	0.1303	0.129	0.1300
0.400	5	2	0.1257	0.1233	0.1210		
0.000	5	0	0.1167	0.1152	0.1118		
-0.400	5	-2	0.1031	0.1024			
0.833	6	5	0.0916	0.0902	0.0908	0.0901	0.0908
0.500	6	3	0.0885	0.0869	0.0857		
0.167	6	1	0.0840	0.0826			
-0.167	6	-1	0.0775	0.0772			
0.857	7	6	0.0675			0.0663	0.0670
0.875	8	7	0.0517			0.0514	0.0514
0.889	9	8	0.0409				0.0407
0.900	10	9	0.0332				0.0331
0.909	11	10	0.0274				0.0274
0.917	12	11	0.0231				0.0230
0.923	13	12	0.0197				0.0196
0.928	14	13	0.0170				0.0169
0.933	15	14	0.0148				0.0148

nances [using Eqs. (21) and (24)] for all low-lying intrashell resonances with the best available quantum calculation employing a high-dimensional Hylleraas or hyperspherical basis and complex rotation techniques. We find for all levels, including the ground state, remarkable agreement at the level of 1% or better. The predictions of our simple model are also in agreement with recent results for the cycle expansion for states near the asymmetric stretch [19]. Note, however, that Eqs. (24) and (21) describe the whole intrashell manifold.

The reason for the accuracy of this extrapolation is not yet fully understood. We note, however, a structural similarity to the dimensional scaling method proposed by Herschbach and co-workers [32]. Dimensional scaling provides quite accurate estimates for energy eigenvalues of He for  $D=3$  by extrapolation for  $D=\infty$ , where the two-electron atom assumes a stationary classical configuration. Corrections in  $1/D$  describe oscillations around the equilibrium. The parameters entering the dimensional-scaling method are the value of the potential and its curvature at the equilibrium, which are related to the actions and the winding numbers. The connection between Eqs. (21) and (24) and dimensional scaling remains to be explained in more detail.

A further test case will be  $H^-$  for which both the asymmetric stretch and the Langmuir orbit are unstable. First results indicate that a similar extrapolation formula

[Eqs (24) and (21)] is also applicable for this case [33]. In order to describe experimental spectra the semiclassical determination of lifetimes or autoionization width [34] will be necessary.

## V. CONCLUSIONS

The stable island around the Langmuir orbit of symmetric doubly excited states can be semiclassically quantized employing quantization of tori winding around the periodic orbit. The quantization predicts energy levels of long-lived classically bound states (decaying only via tunneling or photon emission) residing on the Wannier ridge. These states have very large quantum numbers  $N \geq 5 \times 10^2$  or ( $n_\theta \geq 10^3$ ), i.e., a large number of nodes along the bending mode. The extrapolation of this formula to low-lying states, with the additional constraint imposed that in the limit of the zero-point fluctuation for the bending mode the classical action and winding number of the asymmetric stretch is reproduced, leads to a simple formula for the position of all intrashell ( $N=n$ ) resonances of helium in the  $L=0$  sector. The agreement with sophisticated large-scale quantum calculations is remarkably good. Clearly, this simple model does not yet provide us with predictions for the resonance width. A more detailed test requires accurate quantum calculations for  $N=n \geq 10$ . Progress in this direction [35] is highly desirable.

## ACKNOWLEDGMENTS

We are grateful to R. J. Jelitto for his encouragement and acknowledges helpful discussions with D. Wintgen and C. D. Lin. This work was supported in part by the

National Science Foundation and by the U.S. Department of Energy, Office of Basic Energy Sciences, Division of Chemical Sciences under Contract No. DE-AC05-84OR21400 with Martin Marietta Energy and through Contract No. DE-F605-87ER40361 with the University of Tennessee.

- 
- [1] J. G. Leopold and I. C. Percival, *J. Phys. B* **13**, 1037 (1980); **13**, 1025 (1980).
- [2] M. C. Gutzwiller, *Chaos in Classical and Quantum Mechanics* (Springer, New York, 1990).
- [3] U. Eichmann, V. Lange, and W. Sandner, *Phys. Rev. Lett.* **64**, 274 (1990).
- [4] P. Camus, T. F. Gallagher, J. M. Lecomte, P. Pillet, and J. L. Provost, *Phys. Rev. Lett.* **62**, 2365 (1989).
- [5] P. G. Harris, H. C. Bryant, A. H. Mohagheghi, R. A. Reeder, C. Y. Tang, and J. B. Donahue, *Phys. Rev. A* **42**, 6443 (1990); P. G. Harris, H. C. Bryant, A. H. Mohagheghi, R. A. Reeder, H. Sharifian, C. Y. Tang, H. Tootoochi, J. B. Donahue, C. R. Quick, D. C. Rislove, W. W. Smith, and J. E. Steward, *Phys. Rev. Lett.* **65**, 309 (1990).
- [6] M. Domke *et al.*, *Phys. Rev. Lett.* **66**, 1306 (1991).
- [7] Y. K. Ho, *J. Phys. B* **23**, L71 (1990); *Phys. Rev. A* **34**, 4402 (1986).
- [8] Q. Molina, *Phys. Rev. A* **39**, 3298 (1989).
- [9] N. Koyama, H. Fukuda, T. Motoyama, and M. Matsuzawa, *J. Phys. B* **19**, L331 (1986).
- [10] H. R. Sadeghpour and C. H. Greene, *Phys. Rev. Lett.* **65**, 313 (1990).
- [11] R. P. Madden and K. Codling, *Phys. Rev. Lett.* **10**, 516 (1963).
- [12] J. W. Cooper, U. Fano, and F. Prats, *Phys. Rev. Lett.* **10**, 518 (1963).
- [13] J. L. Van Vleck, *Philos. Mag.* **44**, 842 (1922). See also M. Born, *Atommechanik* (Springer-Verlag, Berlin, 1926).
- [14] G. E. Wesenberg, D. W. Noid, and J. B. Delos, *Chem. Phys. Lett.* **118**, 369 (1985).
- [15] K. Richter and D. Wintgen, *J. Phys. B* **23**, L197 (1990).
- [16] I. Langmuir, *Phys. Rev.* **17**, 339 (1921).
- [17] J. Müller, J. Burgdörfer, and D. W. Noid, *Chem. Phys. Lett.* **178**, 60 (1991).
- [18] J. H. Kim and G. S. Ezra, in *Periodic Orbits and the Classical-Quantum Correspondence for Doubly-Excited States of Two-Electron Atoms*, Proceedings of the Adriatico Research Conference on Quantum Chaos, Trieste, edited by E. Cerdeira and R. Ramaswamy (World Scientific, Singapore, 1991), p. 436.
- [19] G. Ezra, K. Richter, G. Tanner, and D. Wintgen, *J. Phys. B* **24**, L413 (1991).
- [20] C. E. Wulfman, in *Group Theory and Its Application*, edited by E. M. Loebl (Academic, New York, 1971); K. Molmer and K. Taulbjerg, *J. Phys. B* **21**, 1739 (1988). D. R. Herrick and O. Sinanoglu, *Phys. Rev. A* **11**, 97 (1975); D. R. Herrick and M. E. Kellman, *ibid.* **21**, 418 (1980); D. R. Herrick, *ibid.* **22**, 1346 (1980); D. R. Herrick, M. E. Kellmann, and R. D. Poliak, *ibid.* **22**, 1517 (1980); M. E. Kellman and D. R. Herrick, *ibid.* **22**, 1536 (1980).
- [21] J. H. Macek, *J. Phys. B* **1**, 831 (1968).
- [22] J. Müller, X. Yang, and J. Burgdörfer (unpublished).
- [23] J. Müller and J. Burgdörfer, *Phys. Rev. A* **43**, 6027 (1991).
- [24] G. H. Wannier, *Phys. Rev.* **90**, 817 (1953).
- [25] S. Watanabe, *Phys. Rev. A* **36**, 1566 (1987).
- [26] J. M. Rost and J. S. Briggs, *J. Phys. B* **21**, L233 (1988); J. M. Rost, J. S. Briggs, and J. M. Feagin, *Phys. Rev. Lett.* **66**, 1642 (1991).
- [27] D. W. Noid, M. L. Koszykowski, and R. A. Marcus, *J. Chem. Phys.* **73**, 391 (1980).
- [28] W. Sandner (private communication).
- [29] C. D. Lin, *Adv. Mol. Phys.* **22**, 77 (1986).
- [30] F. H. Read, *J. Phys. B* **23**, 951 (1990).
- [31] The accuracy of the extrapolation formulas Eqs. (21) and (24) can be enhanced for low-lying states with the help of a quantum defect. This correction is, however, negligible in the limit of large  $N$ .
- [32] D. R. Herschbach, *J. Chem. Phys.* **84**, 838 (1986); D. J. Doren and D. R. Herschbach, *ibid.* **87**, 433 (1987) and references therein.
- [33] J. Müller and J. Burgdörfer (unpublished).
- [34] Z. Chen and C. D. Lin, *Phys. Rev. A* **40**, 6712 (1989); B. C. Gou, Z. Chen, and C. D. Lin, *ibid.* **43**, 3260 (1991).
- [35] D. Wintgen (private communication).